Vacuum 109 (2014) 216–222

Contents lists available at ScienceDirect

Vacuum

journal homepage: www.elsevier.com/locate/vacuum

# Pulsed vacuum and etching systems: Theoretical design considerations for a pulsed vacuum system and its application to $XeF_2$ etching of Si

Arash Kheyraddini Mousavi [a], Khawar Abbas [a], Mirza Mohammad Mahbube Elahi [b], Edidson Lima [a], Stephen Moya [a], Joseph Daniel Butner [a], Denise Piñon [c], Adeeko Benga [d], Behnam Kheyraddini Mousavi [b], Zayd Chad Leseman [a, *]

[a] University of New Mexico, Department of Mechanical Engineering, Albuquerque, NM 87131, USA
[b] University of New Mexico, Dept. of Electrical & Computer Engineering, Albuquerque, NM 87131, USA
[c] University of New Mexico, Dept. of Chemical and Nuclear Engineering, Albuquerque, NM 87131, USA
[d] University of Texas – San Antonio, Dept. of Mechanical Engineering, San Antonio, TX 78249, USA

ARTICLE INFO

*Article history:*
Received 27 January 2014
Received in revised form
24 July 2014
Accepted 24 July 2014
Available online 1 August 2014

*Keywords:*
Pulsed vacuum
Calibration
$XeF_2$ etching
Analytical modeling
Dynamic modeling

ABSTRACT

Rekindled interest has developed in pulsed vacuum systems due to their use for Xenon Difluoride ($XeF_2$) etching systems and their usefulness in the fabrication of MEMS and nanostructures. Despite numerous applications of pulsed vacuum systems, little information is available in the literature on their design considerations. In this paper mathematical models and their experimental verification are presented for various important design considerations of pulsed vacuum systems. Control of the chambers' pressures and pulse durations are typically the most important design considerations for processes involving pulsed vacuum systems. Pressure sensors give the exact pressure, but accurate chamber volumes are unknown. Thus a methodology is developed for accurate determination of chamber volumes that involves the introduction of a calibrated volume into a chamber. Then it is demonstrated that allowing a known pressure and volume of gas to move between two chambers leads to accurate temporal control of the chambers' pressures. Furthermore, by varying chambers' volumes, configurations, pressures, and the conductances between the chambers it is shown that the pulse duration could be accurately controlled. Though the model and demonstrations are presented in the context of a pulsed $XeF_2$ etching system, they are general and useful for all pulsed vacuum systems.



## 1. Introduction

The use of pulsed vacuum systems is widespread across various manufacturing and processing industries. They are used in numerous industries such as poultry meat and fruit processing/treatments [1,2] and sterilization of medical equipment [3] as well as nanotechnology [4–12]. Despite being used in commercial applications since at least the 1960's not much information is available in the literature on the considerations for designing a pulsed vacuum system. Their more recent use for semiconductor and MEMS device manufacture has brought renewed attention to pulsed vacuum systems. In this work, the design of pulsed vacuum systems is thoroughly studied. During the process of designing and employing the pulsed vacuum system a method for calibration of a vacuum systems volume is described and how the system is used for plasma-less dry etching of Si using Xenon Diflouride ($XeF_2$).

$XeF_2$ was first used to etch silicon in 1978 [13]. Etching with $XeF_2$ has many advantages over traditional silicon etching techniques such as: high selectivity, fast etch rates, isotropic etching, spontaneous etching at room temperature, and has been shown to be useful in the fabrication of MEMS devices [13–15]. Liquid etchants can cause MEMS failure through stiction [4,16–21] and plasma etches can damage them due to ion implantation and temperatures. Plasma etching processes are also limited in their selectivity. The $XeF_2$ etching process removes these complications and helps lead to higher yields in MEMS production [13]. High selectivity has been observed for many metals and masking materials, including $Si_3N_4$, SiC, SiO [13], W, Al, TiN, Cr [5], Au, $SiO_2$, and photoresists [6]. $XeF_2$ can also be used to etch metals like molybdenum, titanium [13], and nickel [7]. Although several custom pulsed $XeF_2$ systems

* Corresponding author.
*E-mail address:* zleseman@unm.edu (Z.C. Leseman).

http://dx.doi.org/10.1016/j.vacuum.2014.07.028
0042-207X/

have been developed in the past [5,22] and some are also available commercially [23,24], to the best knowledge of the authors' the discussions have always been restricted to the etch characteristics and rate dependencies and not on the design characteristics of the system itself. In this paper the authors' present mathematical models and design considerations for a recently developed pulsed $XeF_2$ vacuum system and compare the analytical results to experimental results. Even though the models and the concepts presented in this paper were developed for pulsed $XeF_2$ etching system they hold true for any pulsed vacuum system.

## 2. System design

The simplified schematic diagram of pulsed $XeF_2$ etching system developed for this study is presented in Fig. 1. Logic for the final configuration is presented in subsequent sections. The system is comprised of four stainless steel chambers connected in series and isolated from each other via computer controlled pneumatic valves and a scroll pump.

$XeF_2$ is a white, crystalline chemical first synthesized in 1963 [25] that sublimates at vapor pressures below 3.8 Torr [26]. $XeF_2$ crystals are stored in the 'source chamber' and vacuum is pulled to obtain $XeF_2$ gas; alternatively the source chamber can be replaced by a gas bottle of anhydrous $XeF_2$ or any other chemical process gas (or liquid that evaporates at similar pressures) if required. The remaining three chambers namely: the 'etching chamber', the 'expansion chamber' and the 'dump chamber' are all instrumented with the 0–10 Torr pressure sensors that provide accurate pressure measurements and real time feedback for a custom written computer software to automatically control the etching processes by operating isolation valves. The Baratron pressure sensors used have a 0.001% error of Full Scale. The expansion chamber is installed between the source and the etching chambers and allows a known pressure of $XeF_2$ to be metered into the etching chamber.

The etching chamber is the main chamber of this system and the entire system is built around controlling and maintaining the introduction and withdrawal of the charge gas from this chamber. Samples to be etched are placed in this chamber. Its lid is sealed with a Viton O-ring and is held closed by vacuum. The lid allows access into the etching chamber for sample placement and removal. It also has a provision for the installation of etch depth monitoring via clear glass view port in real time. The dump chamber is a large volume kept under vacuum that enables rapid withdrawal of charge gas (and etch products) from the etching chamber. With the exception of the source chamber, all other chambers can be vented individually by the direct introduction of nitrogen gas. The source chamber is vented through the expansion chamber when required. This was designed intentionally to prevent diluting the $XeF_2$ with nitrogen by accidental venting of source chamber.

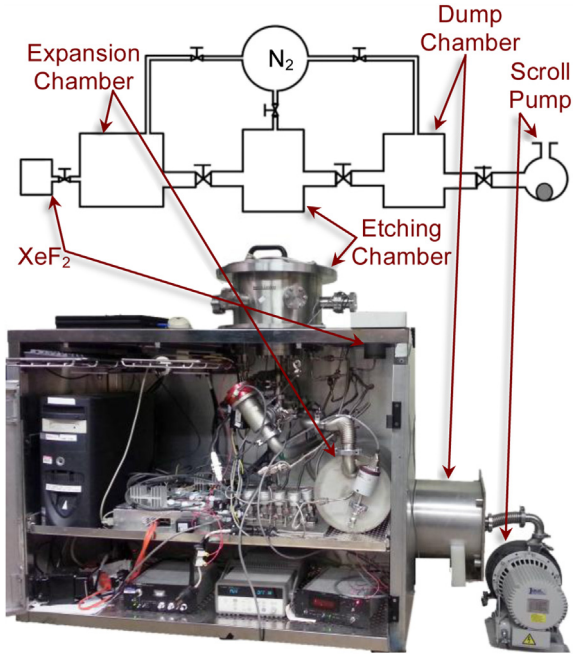


**Fig. 1.** Schematic and picture of pulsed vacuum system used in this work.

During pulsed etching, the expansion chamber is isolated from the source and etching chambers and its pressure is lowered to the base pressure (approximately 10 mTorr for the scroll pump). The expansion chamber is then opened to the source chamber via a pneumatically controlled valve, and $XeF_2$ sublimates into the expansion chamber. The valve to the source chamber is then closed when the expansion chamber reaches the desired pressure, and the etching chamber is brought to the base pressure of the system and again isolated from the pump. The pneumatically controlled valve between the expansion chamber and etching chamber is then opened for a short period of time, allowing a charge of gas to flow into the etching chamber until it achieves the desired etching pressure. This valve is then closed and the system waits for a user-defined etch pulse duration (normally ~60 s or longer) before the pneumatically controlled valve between the etching chamber and dump chamber is opened to remove or quickly 'dump' the gas charge into the dump chamber. The valve between the scroll pump and the dump chamber is always kept opened. The cycle is iterated for a user-defined number of cycles known as pulses.

The base pressure of the system is approximately 10 mTorr, thus the subsequent analyses are relevant to a system operating in the medium vacuum range (i.e. >1 mTorr). With additional considerations the proceeding analyses can be used for high vacuum and ultra-high vacuum systems. Examples of these additional considerations are: outgassing from surfaces, gettering of introduced gas on the surfaces, regurgitation (backstreaming) of the pump(s), and how the gas interacts with the pressure measurement equipment. Finally, catalyzation of surfaces could occur when using reactive gases thereby altering pressure vales. In order to avoid these issues $N_2$ was used in this work.

## 3. Determination of system volumes

Accurate determination and calibration of chamber volumes are extremely important for the experimental verification of any mathematical formulation involving gases at known pressures in chambers with finite volumes. Most real life chambers are not exact rectangles or cylinders as normally depicted in the literature, they are shaped with ease of manufacturing and assembly in mind. Also the existence of input and output ports, tubing lines, nooks, crevices and volumes occupied by the chucks or sample clamps makes the accurate determination of chamber volume by dimensional measurements nearly impossible. Addition of water or any other liquid into a vacuum based system is typically impractical. It may introduce contamination into the system, damage valves or electronics, and trapped gases in the liquid may introduce additional error. More sophisticated techniques for volume measurement of vacuum systems are needed [27]. In this section a novel experimental method for the accurate determination of chamber volumes is introduced. The method is traceable to the calibration standards of length and volume. Though used to calibrate the volume of the pulsed vacuum system this simple method can be used to calibrate any vacuum system.

Consider a system of two unknown volumes connected to each other via a valve that can isolate them from each other. For pulsed vacuum systems, such as one described in the previous section (see Fig. 1), Volume 1 ($V_1$) could represent the volume of etching chamber and Volume 2 ($V_2$) could represent the volume of expansion chamber. Assuming that the etching chamber has been pumped down to the base pressure and the expansion chamber is filled with a gas at some known pressure $P_2$ such that the pressure $P_1 \ll P_2$, then the following conditions will describe this state of the system.

State 1:

$$\begin{array}{llll} P_1 = 0; & V_1 = \text{unknown}; & n_1 = 0; & T_1 = 300\,\text{K}; \\ P_2 = P_2(\textit{known}); & V_2 = \text{unknown}; & n_1 = n\,(\text{unknown}); & T_2 = 300\,\text{K}; \end{array}$$

where $P$, $V$, $n$ and $T$ are the pressure, volume, number of moles of gas and gas temperature, respectively. A subscript of 1 indicates the etching chamber and 2 indicates the expansion chamber. The equation for the state of the system is given by the ideal gas law:

$$P_2V_2 - nRT = 0 \tag{1}$$

where $R$ is the ideal gas constant. Now assume that the valve isolating the two systems is opened and gas is allowed to fill the etching chamber ($V_1$). After the system has achieved equilibrium the new state of the system is:

State 2:

$$\begin{array}{l} P_1 = P_f\left(\text{known}\right);\ V_1 = \text{unknown};\ n_1 = nV_1/(V_1+V_2);\ T_1 = 300\,\text{K}; \\ P_2 = P_f\left(\text{known}\right);\ V_2 = \text{unknown};\ n_2 = nV_2/(V_1+V_2);\ T_2 = 300\,\text{K}; \end{array}$$

where $P_f$ is the final pressure of the gas in both the chambers and is measured from the pressure gages attached to the chambers. Note that the processes here are considered to be isothermal. This state of the system can be described by:

$$P_f(V_1 + V_2) - nRT = 0 \tag{2}$$

From Eqs. (1) and (2) it is clear that we have two equations and three unknowns ($V_1$, $V_2$ and $n$). In order to solve the system another equation is required. This can be achieved by adding a solid block of known volume ($V_0$) to the etching chamber ($V_1$) and thereby reducing the volume of the etching chamber by $V_0$. An alternative could be to add a known volume (additional chamber) to the system thus increasing the volume rather than reducing it. When the expansion chamber is filled with the same pressure $P_2$ as previously and the isolation valve is opened the system attains a new equilibrium pressure $P_f'$ and the state of the system now is:

State 3:

$$\begin{array}{llll} P_1 = P_f'\left(\text{known}\right); & V_1 = \text{unknown}; & n_1 = n(V_1 - V_0)/(V_1 - V_0 + V_2); & T_1 = 300\ \text{K}; \\ P_2 = P_f'\left(\text{known}\right); & V_2 = \text{unknown}; & n_1 = nV_2/(V_1 - V_0 + V_2); & T_2 = 300\ \text{K}; \end{array}$$

In this state the system can now be described by:

$$P_f'(V_1 - V_0 + V_2) - nRT = 0 \tag{3}$$

Eqs. (1)–(3) can now be solved by forward elimination and backward substitution to obtain all the three unknowns:

$$\begin{aligned} n &= \frac{V_0}{RT\left(\frac{1}{P_f} - \frac{1}{P_f'}\right)} \\ V_2 &= \left(\frac{RT}{P_2}\right)n \\ V_1 &= V_0 - V_2 + \left(\frac{RT}{P_f'}\right)n \end{aligned} \tag{4}$$

The method described in the earlier paragraphs of this section and the corresponding equations are now used to calibrate the various chambers of the custom built pulsed $XeF_2$ system with configuration in Fig. 1. The experiment was repeated at various pressures with two different known volume blocks ($V_0$) and each time the volume for etching chamber ($V_1$) and expansion chamber ($V_2$) were determined. Fig. 2 is an example of data obtained using this methodology.

Fig. 2 plots volume versus the initial pressure in the expansion chamber. The data that falls on the lower line is for the etching chamber, $V_1$, and the upper line is for the expansion chamber, $V_2$. The volume calibration experiments have been done in two sets each set with two different volumes for $V_0$. In each set the volume calibration has been performed at 20 different initial pressures of the expansion chamber. All 40 experiments result in similar values for the chamber volumes. Error bars for the data are smaller than the data itself. The horizontal lines in Fig. 2 are a fit through each set of 40 data points. The volume of the etching chamber is determined to be 14.13 L and that of the expansion chamber is 15.12 L.

Measuring the physical volume of the system chambers and implementing the methodology on yet another vacuum system allowed for further verification of the methodology. For example, the expansion and etching chamber volumes were measured using calipers and their volumes were found to be 15.14 L and 14.69 L, respectively. These values are 0.1% lower and 4% higher than their respective calibrated values that were given in the last paragraph. The expansion chamber's measured volume was closer because fewer measurements were made to determine its overall volume than for the etching chamber. Clearly, performing more measurement propagates additional error. The method described in this paper is superior due to its accuracy and because one does not have to disassemble a vacuum system and measure each individual piece. Furthermore, a common method of measuring volumes is to pour a liquid into the volume in question; for many vacuum systems this method can be destructive or at least not preferable to the dry method described in this paper. Two other vacuum systems were tested with this calibration technique. Similar results were found; the method described in this paper is relatively more accurate and easier than other methods.

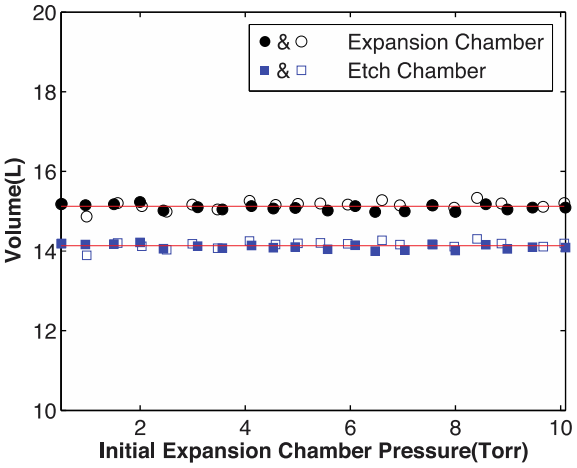


**Fig. 2.** Volume calibration for $V_1$ (circles) and $V_2$ (rectangles).

Using the method described above, the authors have been able to accurately measure multiple volumes of vacuum chambers. Since the length and volume standard can be applied to determine the exact volume of $V_0$ thus this method is traceable to the National Institute of Standards and Technology (NIST).

## 4. Accurate pulse duration

Accurate modeling and control of the pulse duration for a pulsed vacuum system is very important. In a pulsed gas system the gas is let into the process chamber (etching chamber in this case) by opening the inlet isolation valve until the chamber has reached a desired process pressure over a period of time $\Delta t_{start}$. At this point the valve is closed and this pressure is maintained for a certain period of time (pulse duration $\Delta t_{rxn}$). Finally, opening the outlet isolation valve allows for the system to return to its base pressure over a period of time $\Delta t_{finish}$. This process is repeated several times to obtain the desired number of pulses.

For a pulsed $XeF_2$ etching system, the sample placed in the etching chamber will begin etching as soon as the gas is let into the chamber, even before it has reached the desired pressure. Etching will continue until the last of the gas is evacuated from the chamber long after the pressure of the chamber has dropped down from the desired value. In order to control the etching process and determine etch rates under various conditions; it is important that the samples are etched for a 'known' amount of time ($\Delta t_{rxn}$) under 'known' conditions. This implies; having $\Delta t_{rxn} \gg \Delta t_{start}$ and $\Delta t_{rxn} \gg \Delta t_{finish}$. Even though $\Delta t_{rxn}$ is user defined both $\Delta t_{start}$ and $\Delta t_{finish}$ are dependent on the design of the overall system.

In order to formulate a mathematical model that can be used to design these parameters the system is bifurcated into two subsystems. Subsystem 1 is used to describe a set of conditions when the gas is let into the etching chamber from the expansion chamber (Section 4.1) whereas Subsystem 2 is used to describe a set of conditions when the gas is evacuated from the etching chamber (Section 4.2). In other words Subsystems 1 and 2 are used to model the beginning and the end of a single pulse, respectively. Isothermal assumptions are used for both scenarios.

### 4.1. Pulse release to etching chamber

The expansion chamber contains gas at some known pressure $P_1$, whereas the etching chamber is completely evacuated, $P_2 = 0$. The volume for both the chambers is known, measured by the method described in the previous section. The isolation valve between the two chambers is then opened and gas is allowed to flow from the expansion chamber into the etching chamber. Mathematically this system can be described as:

$$\begin{aligned} &\text{for } t<0 && P_1V_1 = nRT \\ &\text{for } t=0 && \begin{cases} P_1 = P_1^i \\ P_2 = 0 \end{cases} \\ &\text{for } t=\infty && P_\infty(V_2+V_1) = nRT \end{aligned} \tag{5}$$

where $P_1^i$ is the initial pressure in the expansion chamber and $P_\infty$ is the pressure in both the expansion and etching chamber after the system has come to equilibrium. From the conservation of mass the relationship between changes in number of moles of the chamber as (6)

$$\dot{n}_1 = -\dot{n}_2 \tag{6}$$

The conductance of the tubing connecting the chambers controls the rate of mass transfer between them. This is shown mathematically in (7), where $C$ is the conductance of the tubing connecting the etching chamber to the expansion chamber.

$$\begin{cases} \dot{n}_1 = -\dfrac{C}{RT}(P_1 - P_2) \\ \dot{n}_2 = \dfrac{C}{RT}(P_1 - P_2) \end{cases} \tag{7}$$

The rate of change of the pressures is controlled by the change in the number of moles in each chamber as shown in (8).

$$\begin{cases} \dot{n}_1 = \dfrac{V_1}{RT}\dfrac{dP_1}{dt} \\ \dot{n}_2 = \dfrac{V_2}{RT}\dfrac{dP_2}{dt} \end{cases} \tag{8}$$

Combining Eqs. (7) and (8) the differential equations governing the pressure of the chambers are found as:

$$\begin{cases} \dot{P}_1 = -\dfrac{C}{V_1}(P_1 - P_2) \\ \dot{P}_2 = \dfrac{C}{V_2}(P_1 - P_2) \end{cases} \tag{9}$$

in which $R$ is the ideal gas constant and $T$ is the absolute temperature of the gas. The system of linearly coupled differential equations of (9), can be solved as:

$$\begin{cases} P_1 = \dfrac{V_1P_1^i}{V_2+V_1}\left(1 + \dfrac{V_2}{V_1}e^{-C\left(\frac{1}{V_2}+\frac{1}{V_1}\right)t}\right) \\ P_2 = \dfrac{V_1P_1^i}{V_2+V_1}\left(1 - e^{-C\left(\frac{1}{V_2}+\frac{1}{V_1}\right)t}\right) \end{cases} \tag{10}$$

From (10) the time constant for Subsystem 1 is:

$$\tau = \frac{1}{C\left(\frac{1}{V_2}+\frac{1}{V_1}\right)} \tag{11}$$

Eq. (11) shows that the time constant for the system is a function of both the system conductance and the chamber volume. By judiciously choosing the system's volumes and conductances the time constant for the pulse rise can be designed. Fig. 3 compares the modeled rise and fall of the etching and expansion chambers with the experimental results from the actual system.

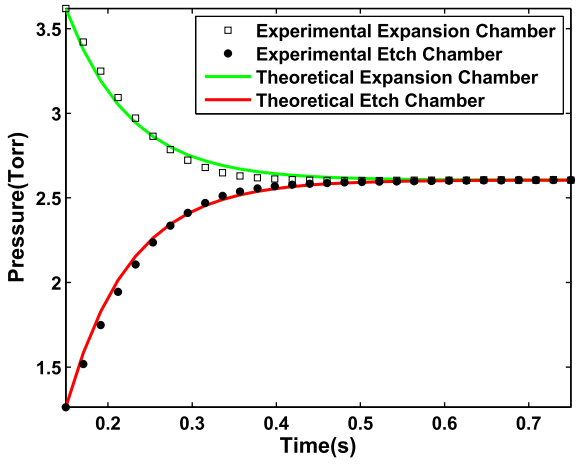


**Fig. 3.** Comparison of the experimental results with the theoretical results of (10).

Experimental results were obtained by evacuating etching chamber to 0.01 Torr (dictated by vacuum system limitation) and filling the expansion chamber with a charge gas to a known initially higher pressure, e.g. 3.62 Torr as in Fig. 4. The valve between the two chambers was then opened and real time pressure change in both chambers was recorded. In Fig. 3 the first 0.15 s has been removed because the valve is still opening and the flow is not yet fully developed and does not obey (10). The time constant for the pulse rise, (11), is 0.08 s. Note that common etching times, $\Delta t_{rxn}$, in the literature commonly range between 30 and 60 s. Making $\tau < 0.3$ s ensures that for common conditions etching chamber's pressure rise accounts for less than 1% of the overall etching time and therefore accounts for a negligible portion of the actual etching time.

The assumption of isothermal expansion is justified when considering the mean free path and velocities of the gas molecules ($N_2$). During one time constant (~0.08 s), more than $0.5^{*}10^5$ collisions occur between the gas molecules and with the surrounding chamber components. This level of collisions allows for the gas molecules to thermalize with the environment on a time scale much shorter than the time constant.

The curves in Fig. 3 are plotted using a value of 91.3 L/sec for $C$. The conductance between the two chambers is mainly dictated by the pipe connecting the chambers. The connection between etching and expansion chamber was composed of two pipes 78.7 cm and 15.2 cm long with diameters of 3.75 cm and 2.54 cm, respectively, and a 22.9 cm long stainless steel flex hose with an outer diameter of 4.9 cm. Thus the pressures and the critical dimensions for this process fall into the transition region between viscous and molecular flows [28]. Calculating $C$ using the viscous pipe flow equation yields 570 L/sec, while for molecular flow yields 4.6 L/sec [28]. The value of 91.3 L/sec falls between these limits as would be expected for a transition flow.

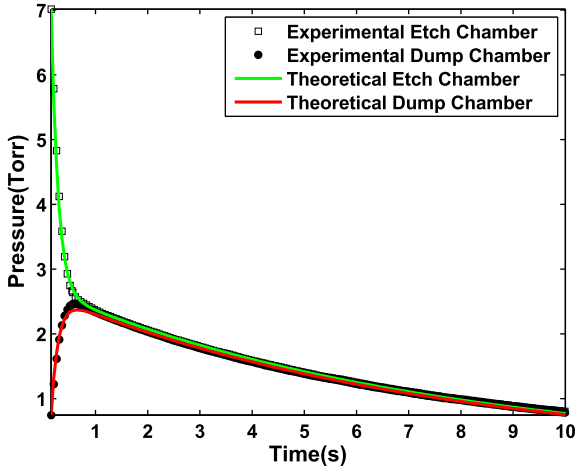


**Fig. 4.** Comparison of the experimental results with the theoretical results of (16).

### 4.2. Pulse dump from etching chamber

Just as it is important to ensure that $\Delta t_{start}$ is negligible in comparison to $\Delta t_{rxn}$ it is also important to ensure that $\Delta t_{finish}$ is negligible as well. An obvious solution is to use a pump with a large enough pumping rate to remove the gases in the etching chamber. However, pumps with relatively large pumping rates are considerably more expensive than those with lower pumping rates if they are even available at all.

Another solution is to connect a tank between the pump and etching chamber that is always open to vacuum. This reservoir tank is used to quickly 'dump' the pressure from etching chamber to a much lower pressure thus reducing the reaction rate considerably while the pump continues to gradually bring the pressure down to the base pressure of the system. With proper design of the volume ratio between the etching and dump chamber one can lower the pressure, and subsequently the reaction rate, to a low enough pressure that nearly all reactions have stopped.

The following is an in-depth discussion on the simulation of the pressure changes in the exhaust process. This process is considerably different than the aforementioned process because there is a pump involved which makes this a nonconservative system. The following analysis mathematically decouples the physics of the dump and etch chambers. This leads to analytical closed form solutions for the exhaust process that allows for easier interpretation of the physics involved. In particular the design is discussed in terms of the time constants for the processes.

The rate of mole transfer from the etching chamber to dump chamber is found in a similar manner as the previous section.

$$\dot{n}_{23} = \frac{C_L}{RT}(P_2 - P_3) \tag{12}$$

where $C_L$ stands for the conductance of the piping that connects the etching chamber to the dump chamber. The subscript 3 refers to dump chamber. $\dot{n}_{23}$ refers to the mole rate from chamber 2 to chamber 3. The rate of mole removal from the dump chamber is dependent on the pump characteristics, which in general depends on the instantaneous pressure on its inlet port. In particular, pumping speed depends logarithmically on the inlet port pressure. Eq. (13) gives the number of moles removed from the dump chamber by the pump per unit time.

$$\dot{n}_p = \frac{P_3}{RT}(k_1 \log P_3 + k_2) \tag{13}$$

where $\dot{n}_p$ refers to mole rate of dumping gas by pump. The rate of change in the number of moles of the etching and dump chamber is:

$$\begin{cases} \dot{n}_2 = -\dot{n}_{23} \\ \dot{n}_3 = \dot{n}_{23} - \dot{n}_p \end{cases} \tag{14}$$

The pressure of the chambers changes directly with the number of moles in the chambers as:

$$\begin{cases} \dot{n}_2 = \dfrac{V_2}{RT}\dot{P}_2 \\ \dot{n}_3 = \dfrac{V_3}{RT}\dot{P}_3 \end{cases} \tag{15}$$

From 14 & 15, the system of differential equations describing the pressure of the chambers is obtained:

$$\begin{cases} \dot{P}_2 = -\dfrac{C_L}{V_2}(P_2 - P_3) \\ \dot{P}_3 = \dfrac{C_L}{V_3}(P_2 - P_3) - \dfrac{P_3}{V_3}(k_1 \log P_3 + k_2) \end{cases} \tag{16}$$

This system of differential equations is solvable only by numerical methods.

Experimental results for the constructed system are compared with the theoretical simulation in Fig. 4. Agreement between the simulation and experimental results is achieved by finding the proper values of the pipe conductance, $C_L$, and the parameters of the pump $k_1$ and $k_2$ using numerical optimization algorithms to achieve proper fit by minimizing the RMS Error. Note that in a less than a few hundred milliseconds the pressure of the etching chamber and dump tank are the same. At this point it is as if the dump chamber does not exist, it behaves as a line with a conductance. This fact allows for the problem to broken into two analytically solvable problems.

One can introduce two time constants to further study the exhaust process that subsequently divides the physics of the problem into two steps. In the first step the chambers are connected to each other (before the two pressures meet) and in the second step the pump lowers the pressure of the two connected chambers (after the two pressures meet). Since the pump is not playing a considerable role in the first step and the pressure difference between chambers is ignorable in the second step the two stages can be considered independent to a good approximation. The ignorable pressure difference between chambers makes it possible to replace the two chambers in the second step with a single chamber of equivalent volume. This results in the coupling of the equations in (16) allowing for theoretical closed form solutions. Although this solution is for a special case the closed form solution obtained allows a deeper understanding of effect of different parameters in the physics of the problem and also allows an easier method to optimize the chamber designs to reach desired time constants for each step.

Subsystem 2 describes the set of conditions for the end of a single pulse, i.e. controls $\Delta t_{\text{finish}}$. Subsystem 2 can be further divided into two subsystems namely Subsystem 2a and Subsystem 2b. In Subsystem 2a the chambers reach the same pressure after the valve opens. In Subsystem 2b the two chambers are considered as a single hybrid dump chamber, which is pumped down to system base pressure. Subsystem 2a is a mass conserving system while 2b is not.

Continuity for Subsystem 2a yield results similar to Eqs. (9)–(11):

$$\begin{cases} \dot{P}_2^* = -\dfrac{C_L}{V_2}\left(P_2^* - P_3^*\right) \\ \dot{P}_3^* = \dfrac{C_L}{V_3}\left(P_2^* - P_3^*\right) \end{cases} \tag{17}$$

which can be solved as

$$\begin{cases} P_2^* = \dfrac{\mathrm{P_2^i}}{V_2 + V_3}\left(V_2 + V_3 \mathrm{e}^{-\mathrm{C_L}\left(\frac{1}{V_2} + \frac{1}{V_3}\right)t}\right) \\ P_3^* = \dfrac{\mathrm{P_2^i} V_2}{V_2 + V_3}\left(1 - \mathrm{e}^{-\mathrm{C_L}\left(\frac{1}{V_2} + \frac{1}{V_3}\right)t}\right) \end{cases} \tag{18}$$

with a time constant of:

$$\tau_a = \frac{1}{\mathrm{C_L}\left(\frac{1}{V_2} + \frac{1}{V_3}\right)} \tag{19}$$

For Subsystem 2b the pressure changes over time can be found by combining the etch and dump chamber into one volume:

$$\dot{P}_3^* = \frac{P_3^*}{V_3 + V_2}\left(k_1 \log P_3^* + k_2\right) \tag{20}$$

The following physical observation makes (20) much simpler to solve and the solution more understandable. As time approaches infinity the flow rate of the pump approaches zero which means at the limit,

$$0 = -\frac{P_\infty}{V_3 + V_2}(k_1 \operatorname{Log} P_\infty + k_2) \tag{21}$$

where $P_\infty$ is the ultimate pressure of the vacuum pump. Solving (21) for $k_2$ we find:

$$k_2 = -k_1 \operatorname{Log} P_\infty \tag{22}$$

Applying (22) to (20) leads to:

$$\dot{P}_3^* = -\frac{k_1 P_3^*}{V_3 + V_2} \log \frac{P_3^*}{P_\infty} \tag{23}$$

which can be solved as

$$\frac{P_3^*}{P_\infty} = \left(\frac{P_0}{P_\infty}\right)^{\exp\left(-\frac{k_1 t}{V \ln 10}\right)} \tag{24}$$

where $P_0 = (V_2/(V_2 + V_3))P_2^i$ is the final pressure of Subsystem 2a expressed as a function of the initial pressure in etch chamber, and $V = V_3 + V_2$. The time constant of Subsystem 2b is:

$$\tau_b = \frac{V \ln 10}{k_1} \ln\left(1 + \frac{1}{-1 + \ln\left(\frac{P_0}{P_\infty}\right)}\right) \tag{25}$$

In an ideal design $P_0$ is designed to be much lower than $P_2^i$. This lowers the etch rate considerably in a short period of time when the valve to dump chamber opens. It is desirable that the pump evacuates the exhaust gasses immediately as well, but since the price of a pump increases drastically with pump flow rate this is not usually practical. The pump constant $k_1$ and $k_2$ are fixed for each pump but proper determination of the time constants using (24) allows proper choice of pump to fit the expected pumping rate for the system.

Again, the goal is to have $\tau_a$ that is approximately 1% or less than a typical pulse duration (30–60 s). From Fig. 4 ta is 0.42 s, which is approximately 1% of a typical etch's duration. A pump with a higher

flow rate will provide a shorter $\tau_b$, which reduces the time to eliminate the gases remaining within the vacuum chamber.

A final note about using Eqs. (16) and (25). When designing a system and using these equations in order to attain proper limits for the behavior of Eqs. (16) and (25) range of values for $k_1$ and $k_2$ should be attained from the manufacturer when possible. As a result of this work it was determined that $k_1$ varied by 28% and $k_2$ by 82% as compared to the manufacturer's manual.

## 5. Summary and conclusions

Dynamic models have been presented for various stages of pulsed vacuum processing. In particular, the case of $XeF_2$ etching of Si was examined. It was determined that the chambers' pressures and pulse durations were the most important parameters involved in this type of pulsed vacuum processing. Therefore, the developed mathematical models focused on the temporal variation of pressure in the associated chambers.

Closed form solutions for the systems of differential equations modeling the temporal variations of pressure (gas flow), were derived. These solutions are valid for situations where pump rates are generally lower than the conductances of associated pipes, connections, and valves that account for the majority of vacuum systems. Eqs. (10), (18), and (24) can be used to study the pressure as a function of time as gases move from one chamber to another. While Eqs. (11), (19), and (25) represent the time constants for different portions of the system. The time constants can be used to gain general insight into which parameters control the introduction and removal of gases from the pulsed vacuum system allowing for optimization of system parameters to meet pulse duration constraints. In this paper the time constants for filling and emptying a pulse was designed and shown to take less than 1% of typical etching durations of $XeF_2$ etching of Si.

Experimental validation was given for the developed equations. However, validation was only possible knowing the exact volumes of the chambers involved. A chamber's pressure is readily available; the exact volumes of the chambers are not. Thus a new methodology for the accurate calibration of vacuum system volumes was developed in which a calibrated volume was introduced into a vacuum chamber while a series of pressures are measured.

## Acknowledgments

Experiments performed were supported by the Office of Basic Energy Sciences, Division of Materials Sciences and Engineering Experimental Program to Stimulate Competitive Research (EPSCoR) under Award# DE - FG02 - 10ER46720. DP acknowledges support from the National Science Foundation, USA – Nano Undergraduate Education program Award 1042062.

## References

[1] Deumier F, Bohuon P, Trystram G, Saber N, Collignan A. Pulsed vacuum brining of poultry meat: experimental study on the impact of vacuum cycles on mass transfer. J Food Eng Jun. 2003;58(1):75–83.
[2] Deng Y, Zhao Y. Effect of pulsed vacuum and ultrasound osmopretreatments on glass transition temperature, texture, microstructure and calcium penetration of dried apples (Fuji). LWT – Food Sci Technol Nov. 2008;41(9):1575–85.
[3] Darmady EM, Drewett SE, Hughes KEA. Survey on prevacuum high-pressure steam sterilizers. J Clin Pathol Mar. 1964;17(2):126–9.
[4] Wu YB, Ding GF, Wang J, Zhang CC, Wang H. Fabrication of low-stress low-stiffness leveraged cantilever beam for bistable mechanism. Microelectron Eng Nov. 2010;87(11):2035–41.
[5] P. B. Chu, J. T. Chen, R. Yeh, G. Lin, J. C. P. Huang, B. A. Warneke, and et al, "Controlled pulse-etching with xenon difluoride," in Proceedings of international solid state sensors and actuators conference (Transducers '97), vol. 1, pp. 665–668.
[6] Muthukumaran P, Stiharu I, Bhat R. Gas-phase xenon difluoride etching of microsystems fabricated through the Mitel 1.5-mu m CMOS process. Can J Electr Comput Eng Can GENIE Electr Inf Jan. 2000;25(1):35–41.
[7] Stevens AAE, Beijerinck HCW. Surface roughness in $XeF_2$ etching of a-Si/c-Si(100). J Vac Sci Technol A Vac Surfaces Film Dec. 2005;23(1):126.
[8] Karbassian F, Mousavi BK, Rajabali S, Talei R, Mohajerzadeh S, Asl-Soleimani E. Formation of luminescent silicon nanowires and porous silicon by metal-assisted electroless etching. J Electron Mater Feb. 2014;43(4):1271–9.
[9] Baghbani Parizi K, Peyvast N, Kheyraddini Mousavi B, Mohajerzadeh S, Fathipour M. Schottky barrier nano-MOSFET with an asymmetrically oxidized source/drain structure. Solid State Electron Jan. 2010;54(1):48–51.
[10] Mousavi A, Atwater M, Mousavi B, Jalalpour M, Taha M, Leseman Z. Mechanical and electrical characterization of entangled networks of carbon nanofibers. Materials (Basel) Jun. 2014;7(6):4845–53.
[11] Atwater MA, Mousavi AK, Leseman ZC, Phillips J. Direct synthesis and characterization of a nonwoven structure comprised of carbon nanofibers. Carbon N Y Jun. 2013;57:363–70.
[12] Alipour Skandani A, Masghouni N, Case SW, Leo DJ, Al-Haik M. Enhanced vibration damping of carbon fibers-ZnO nanorods hybrid composites. Appl Phys Lett Aug. 2012;101(7):073111.
[13] Winters HF, Coburn JW. The etching of silicon with $XeF_2$ vapor. Appl Phys Lett Aug. 1979;34(1):70.
[14] Ibbotson DE, Flamm DL, Mucha JA, Donnelly VM. Comparison of $XeF_2$ and F-atom reactions with Si and $SiO_2$. Appl Phys Lett Jun. 1984;44(12):1129.
[15] Ibbotson DE, Mucha JA, Flamm DL, Cook JM. Plasmaless dry etching of silicon with fluorine-containing compounds. J Appl Phys Nov. 1984;56(10):2939.
[16] Kashamolla MR, Mousavi AK, Leseman ZC. Mode I and mixed mode I and II measurements for stiction failed MEMS devices. In: Micro and nano systems, parts A and B, vol. 12; 2009. p. 25–31.
[17] Leseman ZC, Carlson SP, Mackin TJ. Experimental measurements of the strain energy release rate for stiction-failed microcantilevers using a single-cantilever beam peel test. J Microelectromech Syst Feb. 2007;16(1):38–43.
[18] Leseman ZC, Koppaka SB, Mackin TJ. A fracture mechanics description of stress-wave repair in stiction-failed microcantilevers: theory and experiments. J Microelectromech Syst Aug. 2007;16(4):904–11. http://dx.doi.org/10.1109/JMEMS.2006.883571.
[19] Mousavi AK, Kashamolla MR, Leseman ZC. Improved model for the adhesion of μcantilevers: theory and experiments. J Micromechanics Microengineering Nov. 2013;23(11):115011.
[20] Mousavi AK, Alaie S, Kashamolla MR, Leseman ZC. Nonlinear approach for strain energy release rate in micro cantilevers. In: Micro and nano systems, vol. 10; 2010. p. 51–6.
[21] Kashamolla MR, Goettler DF, Mousavi AK, Leseman ZC. Mode II measurements for stiction failed MEMS devices. In: Micro and nano systems, vol. 10; 2010. p. 63–9.
[22] Chan IWT, Brown KB, Lawson RPW, Robinson AM, Strembicke D. Gas phase pulse etching of silicon for MEMS with xenon difluoride. In: Engineering solutions for the next millennium. 1999 IEEE Canadian conference on electrical and computer engineering (Cat. No. 99TH8411), vol. 3. p. 1637–42.
[23] SPTS Technologies [online]. Available: http://www.spts.com/products/xef2-release-etch/X4.
[24] SAMCO [online]. Available: http://www.samcointl.com/products/01_etching/04_others/vpe-4f.php.
[25] Hyman HH. Noble-gas compounds. Chicago: University of Chicago Press; 1963.
[26] Dagata JA. Chemical processes involved in the etching of silicon by xenon difluoride. J Vac Sci Technol B Microelectron Nanom Struct Sep. 1987;5(5):1495.
[27] Setina J, Erjavec B. Volume determination of a vacuum vessel by pressure rise method. In: Proc. of XIX IMEKO world congress, fundamental and applied metrology, vol. D; 2009. p. 2096–8.
[28] Ohring M. Materials science of thin films. 2nd ed. Academic Press; 2001. p. 794.